International Journal of Multidisciplinary Research and Development
Online ISSN: 2349-4182 Print ISSN: 2349-5979
www.allsubjectjournal.com
Volume 3; Issue 2; February 2016; Page No. 24-28

Trajectory-Simulation of a Charged Particle Beam on Trochoidal Orbit

***[1] Bratati Choudhury, [2] Santanu Paul, [3] Malay Kanti Dey**

[1] Physics Department, Kalna College, Kalna, Burdwan, 713409, West Bengal, India.

[2, 3] Variable Energy Cyclotron Centre, 1/AF Bidhannagar, Kolkata, 700064, West Bengal, India.

Abstract
The trochoidal motion of a charged particle beam in a sector magnet, having a higher magnetic field region separated by a straight boundary from a lower magnetic field region, has been analyzed by simulating the desired magnetic field for trochoidal motion and charged particle trajectories. The trajectories have been simulated by numerically solving the equations of motion of charged particles in the magnetic field. A set of normalized equations of motion are formulated and numerically solved to obtain the reference trajectory, as well as a set of paraxial trajectories. The results show that the gradient of magnetic field near the boundary line of high-field and low-field region appears as an alternating gradient field as far as the trochoidal orbit is concerned. In trochoidal orbit the charged particle beam passes the boundary in opposite directions alternatively and hence the alternating field-gradient provides strong focusing in the vertical direction, apart from the focusing in the horizontal direction present in conventional sector magnets. Using these properties of trochoidal orbits effectively a compact dispersive system with inherent strong vertical focusing can be devised without any separate focusing elements.

Keywords: Charged particle beam, Trochoidal orbit, Alternating Gradient Focusing

1. Introduction
The motion of charged particles in presence of electro-magnetic force has a wide field of application, including particle accelerators, electron microscopes, magnetrons and klystrons, cathode-ray and X-ray tubes, photomultipliers and gas discharges. In many electromagnetic devices the distribution of electromagnetic field results in to complex motion of charged particles. Numerical simulation of the trajectories of charged particles is often necessary to investigate the dynamics in such complex field pattern. In this paper, motion of a beam of charged particles in an external magnetic field having step-function distribution with straight soft-edge transition between the steps has been investigated using single-particle dynamics. In such a field configuration the chaged-particle follows a prolate trochoidal trajectory (figure 1a), i.e., a curve traced by a point in a rotating plane rigidly attached to a circle that rolls without slipping along a line and the point lies outside the circumference of the circle. The trochoidal motion of the charged particle beam is used in many cases, e.g., in injection of low energy charged-particle beam in a sector-focused cyclotron along the hill-valley boundary [1, 2, 3]. Similar orbit is observed in the 360° particle separator described by R. Perry [4, 5], employing two immediately adjacent uniform fields of different strengths, which is basically used to separate different species of ions produced by an ion-source, e.g., H+ and H2+. It can be used in transport of charged particle beam and as a dispersive system also.

2. Equations of Motion
The equation of motion of charged particle [6, 7, 8] in electromagnetic field is governed by Newton's second law $\frac{d\vec{p}}{dt} = \vec{F}$ and Lorentz's force equation $\overrightarrow{F} = q(\vec{E} + \vec{v} \times \vec{B})$, where $\vec{p} = m\vec{v} = m\frac{d\vec{r}}{dt}$ is the momentum, $q, m, \vec{v}$ and $\vec{r}$ are the charge, mass, velocity and position vector of the particle respectively. In the present study electric field ($\vec{E}$) is zero. In magnetic field ($\vec{B}$) it can be written as a set of first order differential equations to be solved simultaneously:

$$\frac{dx}{dt} = v_x, \frac{dy}{dt} = v_y, \frac{dz}{dt} = v_z,$$

$$\frac{dv_x}{dt} = \frac{q}{m}(v_y B_z - v_z B_y),$$

$$\frac{dv_y}{dt} = \frac{q}{m}(v_z B_x - v_x z),$$

$$\frac{dv_z}{dt} = \frac{q}{m}(v_x B_y - v_y B_x) \ldots (1)$$

It is convenient to change the independent variable from time t to the path length (s) along central trajectory [7, 8].
That means,

$$\frac{d}{dt} = \frac{ds}{dt}\frac{d}{ds} = v\frac{d}{ds}.$$

Using this transformation, equations (1) reduces to as given below,

$$\frac{dx}{ds} = \frac{v_x}{v}, \frac{dy}{ds} = \frac{v_y}{v}, \frac{dz}{dt} = \frac{v_z}{v},$$

$$\frac{dv_x}{ds} = \frac{q}{mv}(v_y B_z - v_z B_y).$$

$$\frac{dv_y}{ds} = \frac{q}{mv}(v_z B_x - v_x z).$$

$$\frac{dv_z}{ds} = \frac{q}{mv}(v_x B_y - v_y B_x) \ldots (2)$$

For the sake of computational convenience, we define dimensionless variables

$$\frac{v_x}{v} = \widetilde{v_x}, \frac{v_y}{v} = \widetilde{v_y}, \frac{v_z}{v} = \widetilde{v_z}.$$

Then equations (2) reduce to,

$$\frac{dx}{ds} = \widetilde{v_x}, \frac{dy}{ds} = \widetilde{v_y}, \frac{dz}{dt} = \widetilde{v_z}.$$

$$\frac{d\widetilde{v_x}}{ds} = \frac{q}{mv}(\widetilde{v_y} B_z - \widetilde{v_z} B_y).$$

$$\frac{d\widetilde{v_y}}{ds} = \frac{q}{mv}(\widetilde{v_z} B_x - \widetilde{v_x} z).$$

$\frac{d\tilde{v_z}}{ds} = \frac{q}{mv}(\tilde{v_x}B_y - \tilde{v_y}B_x)$ … (3)

To solve the above written coupled differential equations, we need to evaluate the term $\frac{q}{mv}$. This term is, in fact, inverse of magnetic rigidity $(B\rho)$ of the charged particle. This we see from the circular motion of charged particle in magnetic field satisfying the condition, $\frac{mv^2}{\rho} = qvB$, i.e., $p = qB\rho$. where ρ is the instantaneous radius of curvature. In case of low energy ion beam, extracted from the ion-source with voltage V_{ext}, we can use the non-relativistic equation,

$$\frac{mv^2}{2} = q\,V_{ext}$$
$$v = (2 \cdot \eta \cdot \frac{e}{m_u} \cdot V_{ext})^{0.5}$$

Where $\eta = Q/A$ is called specific charge of the ion, Q is charge state $(q = Qe)$, e is electronic charge, A is mass number, m_u is average mass of a nucleon $(m = A\,m_u)$, V_{ext} is the extraction voltage of the ion source. Then,

$$\frac{q}{mv} = \left(\eta \cdot \frac{e}{m_u} \cdot \frac{1}{2V_{ext}}\right)^{0.5} = c\left(\eta \cdot \frac{e}{m_u c^2} \cdot \frac{1}{2V_{ext}}\right)^{0.5} \text{ … (4)}$$

Here we put the following values, $E_0 = m_u c^2 = 931.5\,MeV$, $c = 2.99794258 \cdot 10^8$ m/sec and V_{ext} in kV, then,

$$\frac{q}{mv} = \frac{1}{B\rho} = 100 \cdot \left(4.824236 \cdot \frac{\eta}{V_{ext}}\right)^{0.5} \text{ … (5)}$$

In relativistic case, the term $\frac{q}{mv}$ can also be represented in terms of kinetic energy (T), as given below. Using relativistic expression of total energy $E^2 = p^2c^2 + {m_0}^2c^4$ and $E = T + m_0c^2$, the momentum of the particle is

$$p = \frac{1}{c}\lfloor T^2 + 2 \cdot T \cdot m_0c^2 \rfloor^{0.5}$$

Then, $\frac{q}{mv} = \frac{q}{p} = \frac{Qe \cdot c}{\lfloor T^2 + 2 \cdot T \cdot m_0c^2 \rfloor^{0.5}}$

Dividing by mass-number A, using $m_0c^2 = A\,E_0$ and expressing energy in MeV unit,

$$\frac{q}{mv} = \frac{1}{B\rho} = \frac{\frac{Qe}{A}c}{1.6 \cdot 10^{-13}\left|\left(\frac{T}{A}\right)^2 + 2 \cdot \left(\frac{T}{A}\right) \cdot E_0\right|^{0.5}}$$

$$\frac{q}{mv} = \frac{\eta \cdot 299.792458}{\left|\left(\frac{T}{A}\right)^2 + 2 \cdot \left(\frac{T}{A}\right) \cdot 931.5\right|^{0.5}} \text{ … (6)}$$

Where T/A is kinetic energy per nucleon in MeV?

3. Magnetic Field Configuration

The magnetic field required for a trochoidal orbit must have different field levels in the transverse direction. In figure (1a) the trochoidal motion of charged particle is shown. A magnetic sector (between lines AB and CD), having higher field level B_{high} for $x < 0$ region (may be called 'hill region') and comparatively lower field level B_{low} for $x > 0$ (may be called 'valley region'), results in to different radius of curvatures (r_h and r_v respectively) for a charged particle with momentum p, to maintain $B\rho = \frac{p}{q} =$ constant. Thus $r_v > r_h$ causes trochoidal motion. Cross-sectional schematic diagram of the magnet is shown in figure (1b), having a step in the pole-gap to shape the magnetic field like a step function with smooth-transition around $x = 0$, as shown in figure (1c).

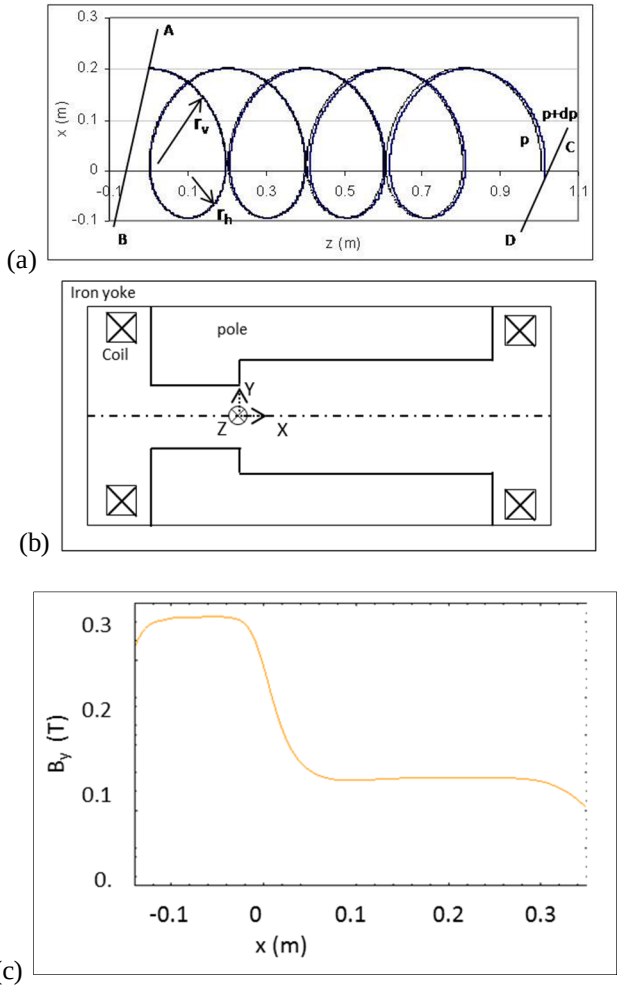

Fig 1: (a) Trochoidal trajectories of two charged particles with momentum p and $p + dp$, (b) Schematic of a magnet with step in pole-gap, (c) Magnetic Field distribution having higher field level B_{high} for $x < 0$ region and comparatively lower field level B_{low} for $x > 0$ region.

Such a magnet, modeled using 3D electromagnetic field calculation software RADIA [9, 10] is shown in figure 2 (a). The 3D magnetic field distribution is shown in figure 2 (b). Such a magnetic field has median plane symmetry, i.e., $B_x = B_z = 0$ at $y = 0$, $B_y(y) = B_y(-y)$, $B_x(y) = -B_x(-y)$ and $B_z(y) = -B_z(-y)$. Inside the magnet $B_z = 0$, except at the entry and exit. From Taylor series expansion of median plane field, we can write, $B_x(y) = (B_x)_{y=0} + y\frac{dB_x}{dy} + \cdots$. Now the first term is zero, due to median plane symmetry. Since, $\nabla \times \vec{B} = \mu_o J = 0$ between the poles of the magnet, so $\frac{dB_x}{dy} = \frac{dB_y}{dx}$.

Hence, $B_x(y) = y\left(\frac{dB_y}{dx}\right)_{y=0}$ … (7a)

Similarly, $B_y(y) = \left(B_y\right)_{y=0} + y\frac{dB_y}{dy}$

From $\nabla . \vec{B} = 0$, we get $\frac{dB_y}{dy} + \frac{dB_x}{dx} = 0$.

Hence, $B_y(y) = \left(B_y\right)_{y=0} - y\frac{dB_x}{dx}$ … (7b)

These relations are used to compute the magnetic field components off the median plane from the median plane field map.

For ease of computation, at the median plane, i.e., at $y = 0$, the field can be fitted with following analytical expression,

$$B_y(x) = B_h - \frac{(B_h - B_v)}{2}(1 + \tanh(a\,x))$$

Where, B_h is the field at high field region (hill), B_v is the field at low field region (valley), a is a parameter which defines the field gradient at the hill-valley transition line and actually depends on the pole gaps in these two regions.

The off-median plane field is given by,

$$B_x(x,y) = -y\frac{(B_h - B_v)}{2}\,a\,(\mathrm{sech}(a\,x))^2$$

$$B_y(x,y) = B_h - \frac{(B_h - B_v)}{2}(1 + \tanh(a\,x)) + 2\,a\,y^2\,(\mathrm{sech}(a\,x))^2\tanh(a\,x) \quad \ldots (8)$$

(a)

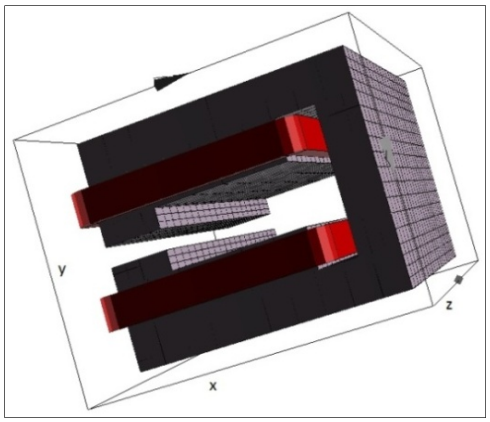

(b)

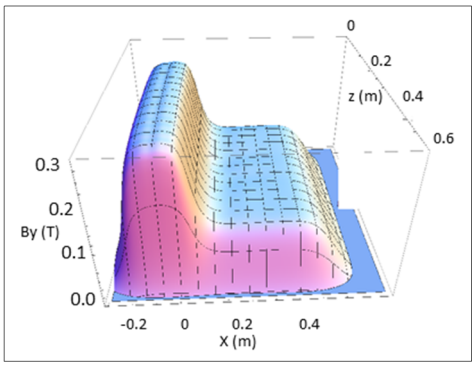

Fig 2: (a) Radia model of the magnet, (b) Median plane magnetic field distribution.

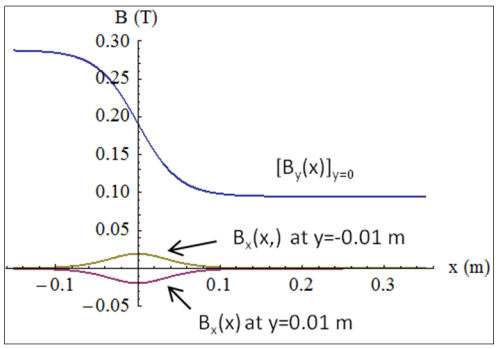

Fig 3: Distribution of field off the mid-plane along the *x*-direction for small values of *y*.

In the high-low transition region the field gradient $\left(\frac{dB_y}{dx}\right)_{y=0}$ is negative, so $B_x(y)$ is negative for $y > 0$ and positive for $y < 0$.

So the force $F_y = v_z B_x$ is focusing (towards median plane) for $v_z > 0$ and defocusing (away from median plane) for $v_z > 0$. In case of trochoidal orbit, therefore, charged-particle beam experiences alternatively focusing and defocusing forces, hence causing net focusing of the beam. Beam crosses the transition field alternatively from one side to another, facing alternatively negative and positive field gradient. This alternating gradient of the field on the path of the beam causes net strong focusing.

4. Results & Discussion

Using the magnetic field defined above the equations of motion are solved to find out the trajectories down the magnet along z direction. Charged particle beam is injected into the low field region (valley), where the radius of curvature (r_v) is larger, gradually enters in to the high field region (hill) with smaller radius of curvature (r_h), thus following a trochoidal path within the magnet.

Following are the results of $\frac{q}{m} = 0.5$, $V_{ext} = 20$kV, $B\rho = 0.029$T-m, emmittance 100-pi-mm-mrad, which is typically the value for a low energy beam from Electron Cyclotron Resonance Ion Source. Eight representative particles are chosen on the boundary of the phase space ellipses, as shown in figure 4, along with the central particle.

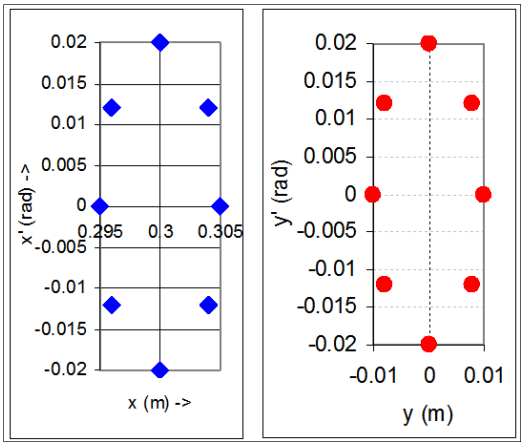

Fig 4: Beam ellipses in transverse directions at the starting point of tracking. Emittance is 100-pi-mm-mrad.

For this beam, the radii of curvature in the $B_h = 0.288$ T and $B_v = 0.095$ T region are $r_v = 0.3$ and $r_h = 0.099$ meters respectively. The central trajectories for momentum p and $p+dp$ are shown in figure 5a and their separation in z direction as a function of path length (s) is shown in figure 5b. This shows the dispersive property of the system.

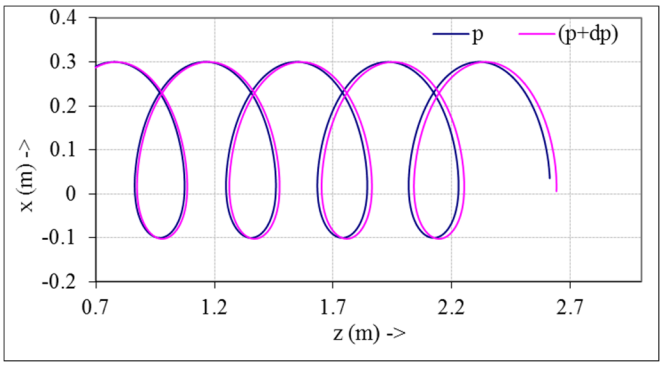

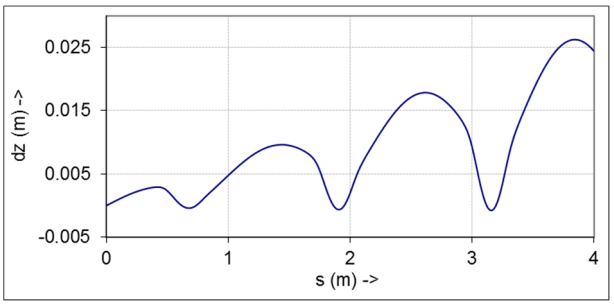

Fig 5: (a) Central particle trajectories in x-z plane (median plane of the magnet) for p and (p+dp). (b) Separation dz, between central trajectories with p and (p+dp), vs. path length s.

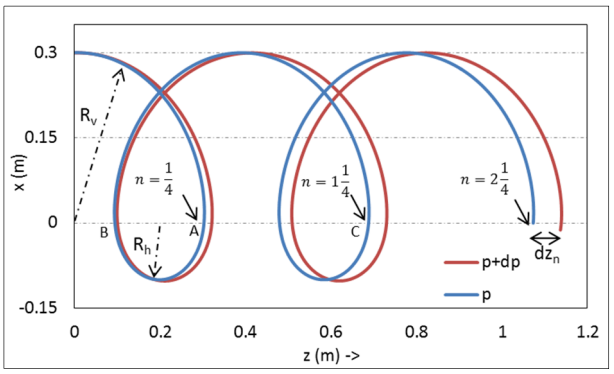

Fig 6: Separation of central trajectories with momenta p and $p + dp$ after n^{Th} turn.

The separation between the central trajectories increases after each successive crossing of valley and hill regions, as shown in figure 6. Let R_v and R_h be the radii of curvature in valley and hill regions for particle with momentum p and $R_v{}'$ and $R_h{}'$ be the same corresponding to momentum$p + dp$. After crossing $\frac{1}{4}th$ of a trochoidal-turn in the valley region, at point A, the separation in z-coordinate is given by,

$$dz = R_v{}' - R_v = \frac{p+dp}{qB_v} - \frac{p}{qB_v} = \frac{dp}{qB_v}$$

After crossing through hill, at point B,

$$dz = (R_v{}' - 2R_h{}') - (R_v - 2R_h)$$
$$dz = (R_v{}' - R_v) - 2(R_h{}' - R_h)$$
$$dz = \frac{dp}{q}\left(\frac{1}{B_v} - \frac{2}{B_h}\right)$$

After crossing $\left(1 + \frac{1}{4}\right)^{\text{Th}}$, i.e., at point C,

$$dz = \frac{dp}{q}\left(\frac{1}{B_v} - \frac{2}{B_h}\right) + 2(R_v{}' - R_v)$$
$$= \frac{dp}{q}\left(\frac{1}{B_v} - \frac{2}{B_h}\right) + 2\frac{dp}{qB_v}$$
$$= \frac{dp}{q}\left(\frac{3}{B_v} - \frac{2}{B_h}\right)$$

In general, after $\left(n + \frac{1}{4}\right)^{\text{Th}}$ turn,

$$(dz)_n = \frac{dp}{q}\left(\frac{2n+1}{B_v} - \frac{2n}{B_h}\right)$$
$$(dz)_n = \frac{dp}{q}\left(\frac{B_h - B_v}{B_v B_h}\right)2n + \frac{dp}{qB_v} \ldots (9)$$

It is shown by eqn. (9) that the z-separation increases with turn number and depends on field ratio$\frac{B_h}{B_v}$.

To study the beam properties, motion of the eight representative particles on the ellipse boundary is to be transformed in to the rotating coordinate fame moving along the central trajectory. As shown in figure 7, let $P_{01}(z01, x01)$ and $P_{02}(z02, x02)$ be two consecutive positions of the central particle on its curved path. Similarly, corresponding positions of another particle moving on a paraxial trajectory be $P_1(z1, x1)$ and$P_2(z2, x2)$.

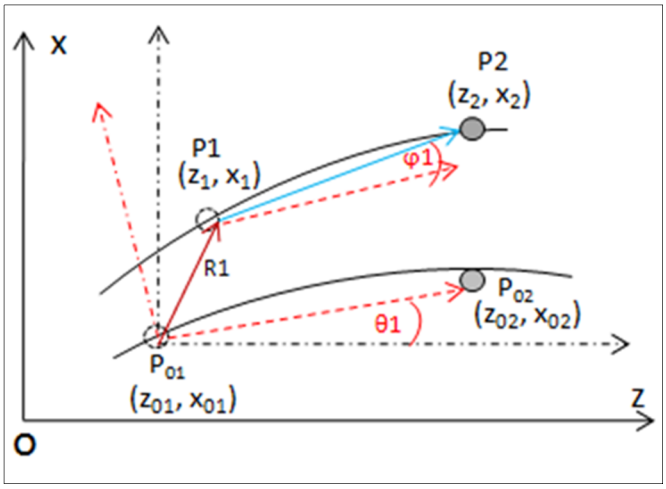

Fig 7: transformation to rotating coordinate system moving with the central trajectory.

The rotation angle of central trajectory is

$$\tan\theta 1 = \frac{x02 - x01}{z02 - z01} \ldots (10)$$

The position vector $R1 \equiv (X_1, Y_1, Z_1)$ of point P_1 with respect to rotating frame at reference particle position $P_{01}$is

$$R1 = \{(z1 - z01)^2 + (x1 - x01)^2 + (y1 - y01)^2\}^{0.5} \ldots (11)$$

Hence transformed coordinate of point $P_1(z1, x1)$ in rotated coordinate system,

$$\begin{pmatrix} Z1 \\ X1 \end{pmatrix} = \begin{pmatrix} \cos\theta 1 & \sin\theta 1 \\ -\sin\theta 1 & \cos\theta 1 \end{pmatrix}\begin{pmatrix} z1 - z01 \\ x1 - x01 \end{pmatrix} \ldots (12)$$

Similarly, transformed coordinate of point $P_2(z2, x2)$ in rotated coordinate system,

$$\begin{pmatrix} Z2 \\ X2 \end{pmatrix} = \begin{pmatrix} \cos\theta 1 & \sin\theta 1 \\ -\sin\theta 1 & \cos\theta 1 \end{pmatrix}\begin{pmatrix} z2 - z01 \\ x2 - x01 \end{pmatrix} \ldots (13)$$

Slope of the arbitrary trajectory $\overrightarrow{P_1P_2}$ in rotating frame,

$$\tan\varphi_1 = \frac{X_2 - X_1}{Z_2 - Z_1} \ldots (14)$$

Using eqn. (12) and (13), we find the transverse position (X_1) and slope $(X_1{}')$ of an arbitrary trajectory with respect to rotating frame,

$$X_1 = -(z1 - z01)\sin\theta 1 + (x1 - x01)\cos\theta 1$$
$$X_1{}' = \frac{X_2 - X_1}{Z_2 - Z_1} = [\{-(z2 - z01)\sin\theta 1 + (x2 - x01)\cos\theta 1\} - \{-(z1 - z01)\sin\theta 1 + (x1 - x01)\cos\theta 1\}] / [\{(z2 - z01)\cos\theta 1 + (x2 - x01)\sin\theta 1\} - \{(z1 - z01)\cos\theta 1 + (x1 - x01)\sin\theta 1\}] \ldots (15)$$

Similarly, in (Y-Z) plane, position and slope are given by,

$$Y_1 = y1 - y01$$

$Y_1 = \frac{Y_2 - Y_1}{Z_2 - Z_1} = \{(y2 - y01) - (y1 - y01)\} / [\{(z2 - z01)\cos\theta 1 + (x2 - x01)\sin\theta 1\} - \{(z1 - z01)\cos\theta 1 + (x1 - x01)\sin\theta 1\}]$ … (16)

Numerical solution of the equations involved gives the transverse trajectories $x(s)$ and $y(s)$, as a function of path length(s), shown in figure 8 and figure 9 respectively. It is evident from the figures that beam is tightly focused in both transverse planes.

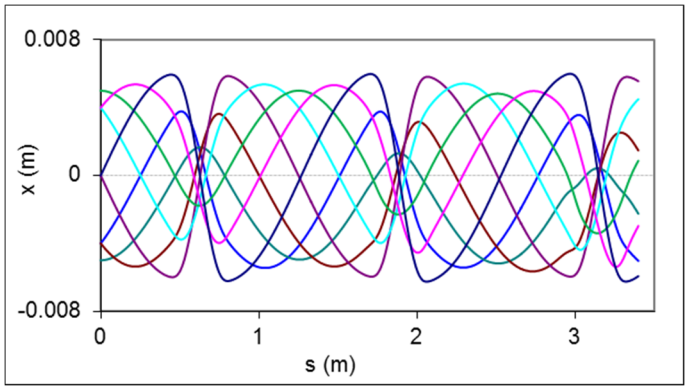

Fig 8: Horizontal trajectories for eight points on ellipse-boundary as a function of path length in rotated frame moving along central trajectory.

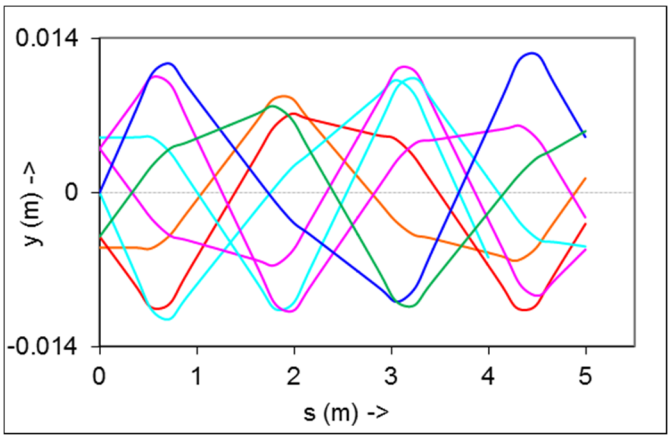

Fig 9: Horizontal trajectories for eight points on ellipse-boundary as a function of path length in rotated frame moving along central trajectory.

5. Conclusion

Numerical simulation has been carried out to study the behavior of trajectories of the charged particle beam in trochoidal orbit. Mathematical formulation has been developed and detailed beam dynamics is investigated in the rotated co-ordinate frame for bunch of particles along with central trajectory. Modeling of a suitable magnetic system having high and low field regions separated by a smooth-transition boundary has also been done using MATHEMATICA based software RADIA. The system may have several advantages like, straight geometry and inherent strong focusing of the beam provided by the field gradient, which happens to be alternating as seen by the beam in trochoidal orbit. The system is shown to have a number of advantages as a compact, strong focusing, high resolving power and still a simple geometry. Such a system may find application in charged-particle beam transport or as a spectrometer.

6. References

1. Kleeven W. Injection and Extraction for Cyclotrons, Proc. CERN Accelerator School CERN 2005, 2006, 012- 271.
2. Mandrillon P. Injection into Cyclotrons, Proc. CERN Accelerator School CERN 1994; 96:02-153.
3. Gladyshev *et al*, VA. Sov. Atom. Ener. (trans.) 1965; 18:3-268.
4. Perry R, A 360° beam separating magnet, R. P. 10, Particle Accelerator Division, Argonne Natl. Lab, 1967.
5. Livingood JJ. The Optics of Dipole Magnets, Academic Press, 1969.
6. Stanley Humphries Principles of Charged Particle Acceleration", PO box 13595, Albuquerque, New Mexico, 87192, (originally published by John Wiley & Sons), 1999.
7. Stanley Humphries Charged Particle Beam, PO box 13595, Albuquerque, New Mexico, 87192, (originally published by John Wiley & Sons), 2002.
8. Rosenzweig JB. Fundamentals of Beam Physics, Oxford University Press, 2003.
9. Elleaume P, Chubar O, Chavanne J. Computing 3D Magnetic Field from Insertion Devices, proc. of the PAC97 Conference, 1997, 3509-3511.
10. Chubar O, Elleaume P, Chavanne J. A 3D Magnetostatics Computer Code for Insertion devices, SRI97 Conference August, J. 1997.